

## Modeling Time to Corrosion Initiation in High-Performance Ferrocement Exposed to Chlorides Environments

S.A.Salih \*, Dr. Maan S. Hassan ; Dr. J. Forth \*\*

Received on: 9/3/2008

Accepted on: 7/8/2008

### Abstract

The applications of a mineral admixture, or a zinc coating to steel surface, or a combination of both are methods used for the corrosion prevention of ferrocement element in this study. Results of a study to evaluate many corrosion protection systems with metakaolin and/or galvanized steel mesh are presented in six U-shaped specimens. Specimens were built to simulate exposure conditions typical for marine environment.

Laboratory data collected along duration of 40 weeks of exposure were used in modeling the cover depth as a function of time to corrosion initiation of the investigated corrosion prevention methods. Methods used to assess the condition of specimens included chloride concentration measurements, and corrosion rates. Model predictions show that the ferrocement specimen of high-performance mortar with metakaolin provides much better level of protection against moisture and chlorides than the conventional specimen, by delay rate of chloride ingress. Application of a galvanized steel mesh causes an elevation of the chloride threshold resulting in an additional increase in the predicted time to corrosion initiation.

**Keywords:** Modeling; Ferrocement; Corrosion; Service life; Durability; Metakaolin, Galvanized steel

### نمذجة الزمن اللازم لبدأ التآكل في الفيروسمنت عالي الاداء المعرض لبيئة الكلور

#### الخلاصة

تم تطبيق نظم مختلفة للحماية ضد تآكل مشبك حديد التسليح المستخدم في السمنت الحديدي (الفيروسمنت). منها المعتمد على المضافات المعدنية، ومنها المعتمد على تغطية سطح المشبك الحديدي بمعدن الزنك (الحديد المكلفن)، ومنها المعتمد على كلا الاثنين. تم تقييم نظم الحماية هذه من خلال تصميم عدد من النماذج المختبرية حيث تم تصميمها لتحاكي الظروف التعرضية المحتملة الحدوث في البيئه البحرية.

استخدمت البيانات المختبرية التي تم جمعها من النماذج على مدى اربعين اسبوع من التعرض الى السائل الملحي، في بناء نموذج (موديل) يحكم الزمن اللازم لبدأ التآكل لنظم الحماية المختلفة التي تم التحري عنها. تشمل الطرق التي تم استخدامها في تقييم نماذج الفحص: قياسات تراكيز ايون الكلور وقياسات معدل تيار التآكل (تقنية مقاومة الاستقطاب الخطي). وينضح من النموذج المذكور ان نماذج الفيروسمنت عالية الاداء التي تم استعمال المضاف المعدني (الميتاكاولين) معها يوفر مستوى افضل من الحماية ضد التآكل من النماذج المرجعية التقليدية وذلك من خلال ابطاء اختراق المحاليل الملحية عبر المونة الى المشبك المعدني. كما ان تغطية المشبك الحديدي بمعدن الزنك يؤدي الى رفع قيمة عتبة الكلور المطلوبة لكسر طبقة اوكسيد الحديد الواقية وبالتالي يؤدي الى اطالة الزمن اللازم لبدأ التآكل.

\* Building and Construction Engineering Department, University of Technology / Baghdad

\*\*School of Civil Engineering University of Leeds, LS29JT, UK

**Nomenclature**

erf	Error function.	Dc	Diffusion coefficient.
tco	Time to corrosion initiation.	Ecorr	The potential of a corroding surface in an electrolyte relative to reference electrode measured under open-circuit conditions.
w/c	Water cement ratio.	GL	Galvanized.
wt.	Weight.	HRWRA	High range water reducing agent.
B	The proportionality constant.	Icorr	Corrosion current.
Ba	Anodic Tafel slop.	L.L.	Corrosion rate.
Bc	Cathodic Tafel slop.	MK	Left leg.
Ci	Initial chloride concentration.	MK&GL	Metakaolin.
Cs	Surface chloride concentration.	RSM	Metakaolin and Galvanized.
C(x,t)	Chloride concentration at time t and depth x.	Ref.	Reinforcing Steel Mesh.
C-S-H	Calcium silicate hydrate.	R.L.	Reference specimen.
Cl-	Chloride ion.	Rp	Right leg.
Cth	Chloride thresholds		Polarization resistance.
CTL-1	Control 1		
CTL-2	Control 2		

**1. Research Significance**

Success of ferrocement as a building material depends on strength and durability under any environmental conditions [1]. Durability is defined as the ability of concrete to resist weathering action, chemical attack, abrasion, and other conditions of service [2]. Ferrocement as a construction material can be successfully used in the construction of many structures such as water tanks, sunshades, secondary roofing slabs, shell and folded plate elements, pipes, and boats [1, 3, 4]. However, if these structures are exposed long-term to sever environment (chloride ions, carbon dioxide, sulfate dioxide, etc.) their service lives will be reduced [5]. Deterioration of mortar is basically related to volume change due to various weathering agents and shrinkage. Deterioration of steel mesh is called corrosion. The steel wire-mesh reinforcement in ferrocement is normally protected against corrosion by the

alkalinity of the mortar and cover. However, carbonation and/or penetration of chloride ions to the mortar cause corrosion to occur. Furthermore, development of any cracks of sufficient width in the mortar component results in a loss of cover thickness and reduces the protection against corrosion [1].

In this study, and due to the importance of durability of a ferrocement, a laboratory service life model is presented for ferrocement structures exposed to chloride-laden environment. Model requirements are the corrosion threshold limit, chloride diffusion constant for initiation of corrosion, mortar properties, reinforcing steel mesh type, and rate of corrosion. The model may be used to predict the service life of new ferrocement construction with normal and high performance ferrocement, and ferrocement with galvanized steel mesh. Thus, the model provides the service life prediction for various corrosion protection systems,

---

\* Building and Construction Engineering Department, University of Technology / Baghdad

\*\*School of Civil Engineering University of Leeds,LS29JT,UK

which are needed for determining the cost-effective solution to corrosion protection of ferrocement structure.

## 2. Service life prediction

Ferrocement may be used as a basic component for concrete structure exposed to marine environments. Durability of ferrocement elements is an important cost issue because of the large number of units involved, and because replacement of any unit already in service can require expensive demolition and reconstruction of associated reinforced concrete work. As a result, design service life requirement for ferrocement units must not be less than design service life of other reinforced units. There are several ways of predicting service life due to corrosion damage of reinforcement in concrete. A simple model for the corrosion of steel in concrete is shown in Figure 1. This service life model for reinforced concrete structures has two stages: *initiation* and *propagation*. This model depicts the time to corrosion initiation and the subsequent deterioration rate. Some structures have been found to follow this model with reasonable accuracy. The initiation time is the length of time until depassivation of the steel reinforcing bars and the initiation of corrosion has occurred. The corrosion rate is controlled by corrosion process kinetics and may increase or decrease. At some point, cracking and spalling occur and the structure is either rehabilitated or has reached the end of its service life and is replaced. Several important factors are needed in order to quantify the deterioration rate: chloride profile, cover depth, carbonation depth, corrosion rate, concrete resistivity, and the environment.

### 2.1 Corrosion Threshold Concentration

Chloride induced corrosion of reinforcing steel is the main cause for deterioration of reinforced concrete structures in marine environments [6, 7, 8]. The use of deicing chemicals and the influence of the coastal region environment were found to be the primary sources of chlorides necessary for the corrosion process to take place. An oxide layer that forms on the steel mesh surface and the high alkalinity of cement paste

normally protects reinforcing steel in mortar. The corrosion process will take place when the passive oxide layer is destroyed. Chloride ions migrating through mortar will cause depassivation of steel mesh after they reach the threshold concentration at the steel mesh-mortar interface. The value of the threshold concentration is of primary importance. It varies for different concrete types. A second theory states that the threshold should not be based on chloride ions only, but rather on a ratio of chloride to hydroxyl ions [9, 10]. According to Verbeck and Hausmann [11, 12], ratios above 0.6 indicate high probability of active corrosion, while ratios below 0.6 are considered to be normal. It can easily be deduced that not only an increase in chloride ion concentration will cause the ratio to increase, but a decrease in hydroxyl ion concentration as well. However, accurate determination of hydroxyl ion concentration is difficult, especially at high concrete pH levels.

### 2.2 Cady-Weyers Deterioration Model

The average service life of concrete structure exposed to marine environment in the United States, including rehabilitation and the component replacement, was estimated to be 70 years. Major rehabilitation of a bridge takes place when the structure is about 35 years old [13]. The design life for buildings and other structures in Europe is 50 years, while bridges are expected to last 120 years [9, 10]. Such long durability requirement presents a difficult materials selection and performance prediction challenge. Under these conditions predicting the service life of any structural unit, which includes present knowledge of their deteriorated condition, became an important subject in making the most cost-effective decisions concerning future management of these structures. A corrosion deterioration model for concrete structures exposed to chloride environment was proposed by Cady and Weyers, see Figure 2[14]. This general representation of deterioration versus time relationship can be divided into three stages: *diffusion*, *corrosion*, and

**deterioration.** The diffusion period is the time when chloride ions penetrate the concrete cover until their concentration, at a rebar level, reaches the corrosion threshold level. The second period in this model is called the corrosion period. In this stage the corrosion of the reinforcing steel initiates and progresses until first cracking occurs. Factors such as bar size, its spacing, and concrete cover above the steel determine whether incline or delamination cracking occurs [15]. The last period in the Cady-Weyers deterioration model is the deterioration phase. In this period, the concrete structure continues to deteriorate until the time when repair or rehabilitation is required. Factors such as delaminations, spalling, patches, and cracking influence decisions regarding the time of repair or rehabilitation.

### 2.3 Complexity of Corrosion Process

Corrosion is an electrochemical process, and strongly dependent on environmental factors (temperature, relative humidity, rainfall) and properties of concrete structure. These factors act simultaneously on the corrosion process in the service conditions. The influence of these factors on the corrosion process should be considered as an interaction among them. The interaction model for corrosion has not been sufficiently studied due to the lack of the long-term corrosion data in the field. Most of the research work in accelerated corrosion tests is limited to the effects of the individual variable. In fact, these factors cannot be separated or isolated from each other in the service conditions. It is necessary to develop an interaction model to characterize the corrosion process based on long-term corrosion tests. Therefore, the service life of a reinforced concrete structure in different environmental conditions can be better predicted [16, 17]. This study concentrates on a diffusion period of the Cady-Weyers deterioration model, which also is the maintenance free period in their last model [13, 14]. Based on Figure 2, it is clear that one method to extend time to rehabilitation is to extend the time to corrosion initiation. It can be achieved by reducing the diffusion rate or by

increasing the chloride threshold level. Mineral admixtures can accomplish reduction of the diffusion rate, while chloride threshold level can be elevated with metallic coating. The proposed model uses laboratory data, and estimates field performance of “new low permeable mortar” in high performance ferrocement.

### 3. Materials and mixes:

Ordinary Portland cement was used in this study. Table 1 shows the chemical composition of this type of cement.

#### 3.1 Specimen Design

It was suggested to use the specimen of a shape as shown in Figure 3 to be the ferrocement structural element of this study. Each specimen, was 0.96 m high and horizontal dimensions of 0.46 m by 0.4m, and was designed to simulate four exposure conditions: wetted surface (horizontal zone), wetted vertical surfaces of members (vertical zone), tidal zone, and immersed zone. The immersed zone covered an area from the bottom of specimens' legs to the height of 200 mm. The tidal zone was 200 mm to 400 mm from the bottom of specimens' legs. A vertical surface area above 400 mm from the bottom of a specimen corresponded to the vertical zone, and the horizontal zone is the top surface area of the specimen. The constant design parameters for these specimens are a 100-110 mm flow; all specimens had 14.3 mm mesh reinforcing cover depth and had been exposed to a 6%, by weight, sodium chloride wetting solution. The variable design parameters are:

- Configuration of the reinforcing steel mesh (RSM).
- Type of reinforcing steel mesh.
- Cementitious material.

#### 3.2 Reinforcing Steel Mesh

A wire mesh was used to reinforce the specimen. The wire mesh cover for all specimens was 14.3 mm. To study the effect of wire mesh configuration or macrocell actions on corrosion performance, three configurations were adopted: -

**Type I** - RSM electrically connected in both legs, (same mesh for vertical, tidal, and immersed zones, (see Figure 4).

**Type II** - RSM electrically disconnected in both legs, (see Figure 5).

**Type III** -RSM electrically disconnected in the right leg and connected in the left leg (same mesh for vertical, tidal, and immersed zones, see Figure 6). Also two types of steel wire mesh were used throughout this study. Some specimens were reinforced with normal steel wire mesh and others were reinforced with galvanized steel wire mesh to study the effect of metallic coating on corrosion.

### 3.3 Cementitious material

Mortar mixes were used for all specimens with mix proportions of 1:2 (cement: sand by weight) with a flow of 100 – 110 mm. To improve the quality of the mortar mixes two types of admixture were used. A 0.7% by weight of cement of a high range water reducing agent was used for some mixes. Also a 10% by wt. of metakaolin as a partial replacement of cement was used to improve the durability of ferrocement mortar. Table 2 shows the details of the experimental program.

### 3.4 Specimens Casting and Curing

Discontinuity of the mesh was achieved by employing epoxy coating for the overlap part of steel mesh that was used in place of regular mesh steel reinforcement in the transition areas between selected exposure zones. These overlap meshes are connected to the mesh steel reinforcement with plastic ties to ensure that the steel mesh are isolated from each other. Specimens were cast in plywood forms, which were carefully cleaned and oiled before each mortar placement. Placing of mortar was done in three layers. While placing mortar; a vibrator table was used in each layer to achieve good compaction especially in the specimens' legs. Specimens were wet cured in the forms for five days. After removing the specimens from the forms they were kept in moisture condition and covered with plastic nylon for additional 23 days of wet curing. Ferrocement specimens, after being removed from the wooden forms, are presented in Figure 7. After 28 days of wet

curing, specimens were air-dried in the laboratory for a minimum of 30 days. During that time the specimens were prepared for wet-dry cycles. Then all specimens were placed into a 0.5 m deep tank and exposed to wet-dry cycles. Figure 8 shows all six specimens in the tank.

each layer to achieve good compaction especially in the specimens' legs. Specimens were wet cured in the forms for five days. After removing the specimens from the forms they were kept in moisture condition and covered with plastic nylon for additional 23 days of wet curing. Ferrocement specimens, after being removed from the wooden forms, are presented in Figure 7. After 28 days of wet curing, specimens were air-dried in the laboratory for a minimum of 30 days. During that time the specimens were prepared for wet-dry cycles. Then all specimens were placed into a 0.5 m deep tank and exposed to wet-dry cycles. Figure 8 shows all six specimens in the tank.

### 3.5 Exposure Conditions

Specimens were kept indoors and exposed to wet-dry ponding cycles. Each cycle was four weeks in duration and was divided into two stages. In the first stage (two weeks) the wetting solution was at high tide level (400 mm from the bottom of a specimen), thus the tidal zone and the immersed zone areas were covered with NaCl solution, and the horizontal and vertical zones of the specimen were allowed to air dry. In the second stage the wetting solution, while at low tide level (water level at 200 mm from the bottom of a specimen), was pumped to the top of a specimen, thus wetting the specimen surfaces in the horizontal and vertical zones. At the same time surfaces in the tidal zone were allowed to air dry. The immersed zone is constantly submerged in the NaCl solution. The wetting solution used in the study is 6% sodium chloride by weight. After approximately 40 weeks of wet-dry cycles, the specimens were removed from the tanks and moved outdoors.

### 3.6 Evaluation Methods

The objective of this study was to investigate the durability (corrosion

behavior) of ferrocement structural element. Specimens were made with different types of mortars (Normal mortars, mortar with chemical admixture, and with metakaolin) and different type of wire mesh (Normal and galvanized wire mesh). Methods were used to assess specimen performance included the rate of chloride ingress, and corrosion rate measurements.

#### 4. Results and Discussion:

##### 4.1 Corrosion Rates

Corrosion rates were measured at each exposure zone and each leg, for a total of 7 different locations per specimen. Corrosion rate data were determined by using Stern Geary equation ( $I_{rate} = B / (R_p * A)$ ), for reinforcement steel mesh of all specimen. Results are shown in Figures 9-12. Test results show that the corrosion rates in the horizontal zone, Figure 9 slightly increase with age of exposure. While the same behavior is observed, for other zones, see Figures 10-12, with the exception of little shifting to the lower value for right legs of High-Performance ferrocement specimens compare with corrosion rates of left legs. This behavior is mostly because of macrocell action.

The corrosion rate results, as shown in Figures 9-12 indicate that the control specimens are in an active region of corrosion for all exposure types, since the corrosion rates were higher than  $0.2 \mu A/cm^2$  [18, 19, 20], while corrosion rates for MK, GL, and MK&GL specimens still in passive condition. It is also shown that there are little improvements for MK&GL specimen as compared with GL specimen rather than significant improvement for GL as compared with MK or HRWRA specimen. This is indicated that the performance of protection system by using galvanized steel mesh was better than the performance of MK specimen, which used the mineral admixture (metakaolin) only. A probable explanation of these results is that the cover of steel mesh in ferrocement is

usually small value and then the defense against corrosion by protection of steel itself by coating with zinc has higher effectiveness than the improvement of mortar quality of the cover depth of steel mesh in ferrocement.

##### 4.2 Chlorides

Chloride concentrations were determined for all mortar types used for ferrocement specimens. After 40 weeks of ponding, mortar powder samples were collected from three depths of small mortar blocks which were placed in vertical, tidal, and immersed zones for this purpose. Mortar powder samples were collected from three depths for each zone, 5, 10, and 15 mm. The chloride concentrations of the powders samples were obtained using the method of acid extraction. Once the chloride ion concentrations are measured, diffusion coefficients are calculated for all specimen types. The calculations are performed in accordance with the Fick's second law of diffusion; see Equation 1[21].

$$c_{(x,t)} = c_s - (c_s - c_i) \operatorname{erf} \left( \frac{x}{\sqrt{4D_c t}} \right) \quad (1)$$

Where

$C_{(x,t)}$  = chloride concentration measured at depth  $x$  and exposure time  $t$ , mass%.  $C_s$  = surface chloride concentration at the interface between the exposure liquid and test specimen, mass%.  $C_i$  = Initial chloride concentration of the cementitious mixture prior to submersion in the exposure solution, mass%.  $X$  = depth below the exposed surface (mm).  $D_c$  = Diffusion coefficient.  $(mm^2/year)t$  = the exposure time (year), and erf = the error function given in standard mathematical reference books[22], also included as a library function in most electronic software programs. Since the chloride concentrations were measured at three depths the "Least Squares Fit Concept", as described by Weyers et al. [23], was employed to obtain the best fit of the diffusion coefficient. Calculated diffusion

coefficients corresponding to the minimum of the sum of squared errors, after 40 weeks of laboratory exposure, are presented in Table 3. As shown in Table 3,

### 5.0 Modeling the Time to Corrosion Initiation

Service lives of control, and high-performance ferrocement with or without galvanized steel mesh were determined from the results of the laboratory investigations.

The powdered mortar samples from the top 3 to 4 mm were discarded due to the high variability of chloride content close to the surface.

Data collected from the laboratory investigations were used to determine time to corrosion initiation for all ferrocement types. Calculations were performed by an interactive solution of Equation 1 and solving it for time, *t*. The following four parameters were used to solve Equation 1: chloride concentration threshold, *C*(*x*, *t*), surface concentration, *C<sub>s</sub>*, reinforcing steel mesh cover depth, *x*, and diffusion coefficient, *D<sub>c</sub>*. Equation 1 is rewritten as follows:-

$$t_{co} = \frac{x^2}{4 D_c \left[ \operatorname{erf}^{-1} \left( \frac{C(x,t) - C_s}{C_s - C_i} \right) \right]^2} \quad (2)$$

Corrosion initiation time as a function of cover depth of steel mesh, for control (conventional), and high-performance ferrocement with or without galvanized steel mesh, is presented in Figure 13.

Figure 13 shows the difference between these various protection systems for corrosion in ferrocement, for vertical zone (as an example). It is clearly indicated that there is a significant improvement with different degree from the control specimen. Table 4 presents degree of improvement (in extension of time to corrosion initiation) for each system with respect to control specimen.

after 40 weeks of ponding the lowest chloride diffusion level is observed in the MK specimens, higher values are observed in the control specimens

Table 4 shows that the protection system using galvanized steel mesh has the higher effectiveness in the extension of the predicted time to corrosion initiation, and then time to corrosion damage and rehabilitation. This result agrees with the results of corrosion rates (see Figure 10).

### 6. Conclusions

Based on the experimental work and test results of this study, the following conclusions can be drawn:

- 1- Comparing the four exposure conditions, the low corrosion rates in the immersed zone are most likely due to higher moisture content, which limits the supply of oxygen. The higher value observed in the vertical zone is related to the availability of oxygen supplied to the steel mesh surface. It seems that the arrival of oxygen to steel mesh surface is the main factor in the corrosion process of ferrocement, therefore it is considered as a cathode control process.
- 2- Results of chloride testing indicate that the amount of chlorides present at the bar level is more than sufficient for corrosion to occur for the control specimens; however, it is still low for the specimens with high-performance mortar. Based on chloride data it appears that the specimens with metakaolin are the least prone to chloride ingress. Specimens with chemical admixture (HRWRA) will allow for greater intrusion of chlorides, but still much less than the controls. This is confirmed by comparing diffusion coefficients: they are more than ten times lower for the specimens made with mortar with mineral admixtures, as compared to the controls.
- 3- High-performance mortars provide much better level of protection against moisture and chlorides than the conventional ferrocement mortar (control) alone. Application of a galvanized steel mesh causes the beneficial elevation of the chloride threshold and results in an

increase in time to corrosion initiation and then time to corrosion damage.

4- The model clearly indicates that in case of little value cover depth, which is a common case in ferrocement, neither conventional mortar ( $w/c=0.52$ ) nor high-performance mortar, can play the required useful role to prevent the ingress of chloride inside to the level of steel mesh.

#### 7. Recommendations for Further Research

Due to the importance of this subject and to continue studying this field, the following recommendations are put forward:

1. It is recommended that the specimens be further exposed to chloride ions and annual monitoring be continued until corrosion cracking has occurred to better estimate the service life extension provided by mineral admixtures and/or galvanized steel mesh used in the ferrocement components.

2.0 Even though the presented  $D_c$ ,  $C_s$  and Fick's second law provide good basis for the analysis, field studies are needed to have a better representation and validation of ferrocement in marine conditions. Also, calculated time needed to corrosion initiation for ferrocement with mineral admixtures, as well as the elevated corrosion threshold levels provided by zinc-coated need to be verified by field study.

#### References

- [1] American Concrete Institute (ACI). Cement and concrete terminology. ACI Manual of concrete practice. ACI Committee 116R; 2001
- [2] Neville AM. Properties of concrete. New York: John Wiley & Sons, 1997.
- [3] Tatsa EZ. Ferrocement in housing – the future. Nedwell PJ, Swamy RN, editor. Proceedings Ferrocement Symposium. London, 1994. p. 55-67.
- [4] Pama RP. Ferrocement – an overview. Nedwell PJ, Swamy RN, editor. Proceedings Ferrocement Symposium. London, 1994. p. 3-16.
- [5] ] Hassan M.S. Laboratory simulation of time to corrosion in high-performance ferrocement exposed to chlorides. PhD

Thesis, Baghdad, University of Technology, 2007.

- [6] Page CL, Treadaway KWJ. Aspects of the electrochemistry of steel in concrete. *Nature* 1982;297:109-114.
- [7] Glass GK, Hassanein AM, Buenfeld NR. Monitoring the passivity of steel in concrete induced by cathodic protection. *Corrosion Science* 1997; 39(8):1451-1458.
- [8] Leek DS. The passivity of steel in concrete. *Quarterly Journal of Engineering Geology* 1991; 24:55-66.
- [9] Breit W. Critical corrosion inducing chloride content—state of the art (Part I). *Betontechnische Berichte* 1998;7:442–449.
- [10] Thomas M. Chloride thresholds in marine concrete. *Cem Concr Res* 1996; 26(4):513-519.
- [11] Verbeck GJ. Mechanisms of corrosion of steel in concrete. *Corrosion of Metals in Concrete*, ACI SP-49 1975:21-38.
- [12] Haussmann DA. Steel corrosion in concrete; How dose it occur? *Materials Protection* 1967; 6(11): 19-23.
- [13] Cady PD, Weyers RE. Predicting service life of concrete bridge decks subject to reinforcement corrosion. *ASTM Special Technical Publication* 1992;1137:328-338.
- [14] Cady PD, Weyers RE. Deterioration rates of concrete bridge decks. *Journal of Transportation Engineering* 1984; 110(1):34- 44.
- [15] Bazant ZP. Physical model for steel corrosion in concrete sea structures—theory. *ASCE Journal of the Structural division* 1979;105(6):1137-1153.
- [16] American Concrete Institute (ACI). Corrosion of metals in concrete. ACI Manual of concrete practice. ACI Committee 222R-01; 2002.
- [17] Liu Y. Modeling the time-to-corrosion cracking of the cover concrete in chloride contaminated reinforced concrete structures. PhD thesis. Blacksburg, Virginia Polytechnic Institute and State University, 1996.
- [18] Raupach M, Elsener B, Polder R, Mietz J. Corrosion of reinforcement in concrete: Mechanisms, monitoring, inhibitors and rehabilitation



techniques. Cambridge England: Woodhead publishing limited, 2007.  
 [19] Broomfield JP. Corrosion of steel in concrete: understanding, investigation, and repair. London: E. & F.N. Spon, 2007.  
 [20] The Concrete Society. Electrochemical tests for reinforcement corrosion. Technical Report 60, Camberley, 2004.  
 [21] American Society for Testing and Materials. ASTM Standard test method for determining the apparent chloride

diffusion coefficient of cementitious mixtures by bulk diffusion. Philadelphia: American Society for Testing and Materials ASTM C 1556-03; 2003.  
 [22] Beyer, W. H., ed., CRC Handbook of Mathematical Sciences, 5th Edition, CRC Press, Boca Raton, FL, 1978.  
 [23] Prowell BD, Weyers RE, Al-Qadi IL. Concrete bridge protection and rehabilitation: chemical and physical techniques, service life estimates. Virginia Polytechnic Institute SHRP-S-668; 1994.

**Table (1) Chemical composition of cement.**

Oxide composition	Content Percent
CaO	61.09
SiO <sub>2</sub>	20.1
Al <sub>2</sub> O <sub>3</sub>	5.75
Fe <sub>2</sub> O <sub>3</sub>	3.01
SO <sub>3</sub>	2.45
MgO	2.01
K <sub>2</sub> O	0.60
Na <sub>2</sub> O	0.22
(Na <sub>2</sub> O+0.658K <sub>2</sub> O)	0.6148
L.O.I.	2.21
I.R.	1.47
L.S.F.	0.92

**Table (2) Details of Experimental Program.**

Specimen designation	Mix Proportion	w/c Ratio	Type of steel mesh	Type of admixture			Electrical steel configuration	Type and age of test		Exposure conditions
				HRWRA % by wt of cement	MK % by wt of cement	Chromium Trioxide with		Corrosion rate	Chloride concentration	
CTL-1	1 : 2 (cement: sand) and Flow 100-110 mm	0.52	Normal	-	-	-	Type 1	At age 20, 30, and 40 weeks of ponding	At age 20, 30, and 40 weeks of ponding	Horizontal, vertical, tidal and immersed
CTL-2		0.52	Normal	-	-	-	Type 2			
HRWR A		0.34	Normal	0.7	-	-	Type 3			
MK		0.38	Normal	0.7	10	-	Type 3			

GL		0.34	Galvanized	0.7	-	100 ppm	Type 3			
MK&GL		0.38	Galvanized	0.7	10	100 ppm	Type 3			

Table (3) Diffusion Coefficients Based on Chloride Data after 40 Weeks of Exposure.

Specimen	Diffusion Coefficients [mm <sup>2</sup> /year]		
	Vertical Zone	Tidal Zone	Immersed Zone
Control	253	412	370
HRWRA	29.39	37.23	37.49
MK	12.76	23.94	33.88

Table (4) Degree of Improvement for Different system of Protection (at Cover Depth = 15 mm).

Specimen (Protection system)	Degree of Improvement (Times control value)
HRWRA	12.9
MK	29.78
GL	56.21
MK&GL	129.47

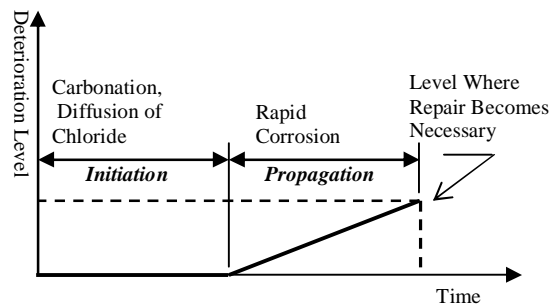


Figure (1) Simple corrosion deterioration models

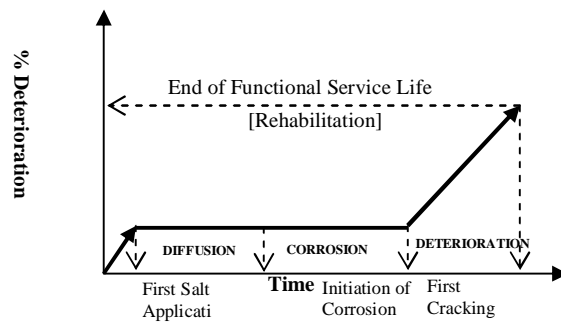


Figure (2) Cady-Weyers Deterioration Model [14].

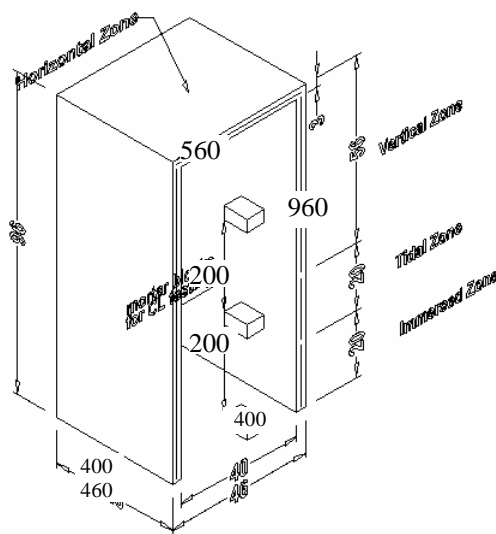


Figure 3 Typical Specimen Notes: All dimensions in (mm). Ferrocement thickness=3 cm..

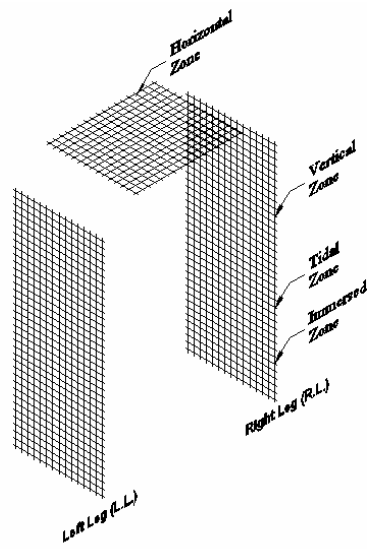


Figure 4 Type I – RSM electrically connected in both legs.

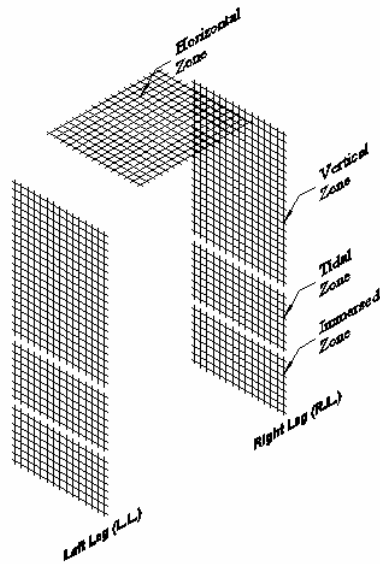


Figure 5 Type II – RSM electrically disconnected in both legs.

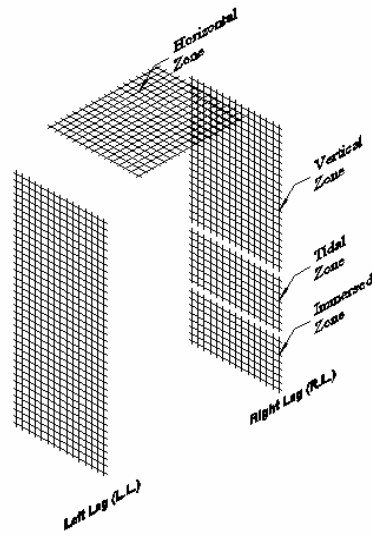


Figure (6) Type III – RSM electrically disconnected in right leg & electrically connected in left leg.



Figure (7) Typical Specimen after removal from the forms



Figure (8) Specimens placed into the tank.

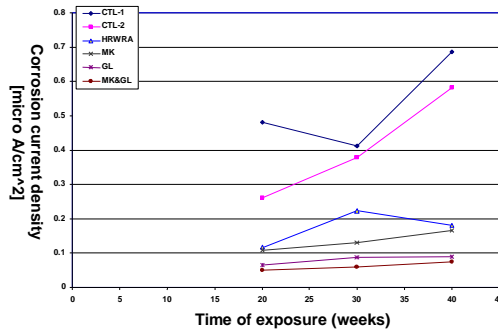


Figure (9) Corrosion Rates in the Horizontal Exposure Zone for all Specimens.

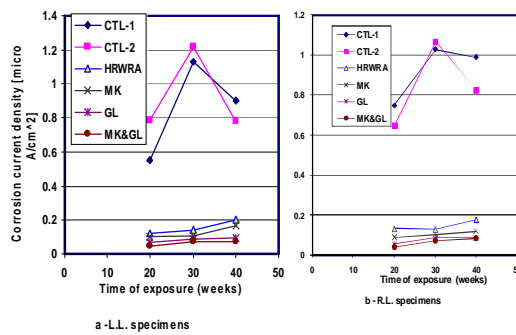


Figure (10) Corrosion Rates in the Vertical Exposure Zone for all Specimens.

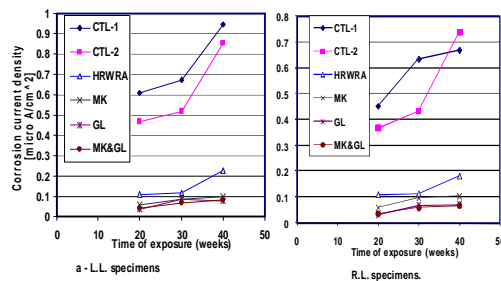


Figure (11) Corrosion Rates in the Tidal exposure Zone for all Specimens.

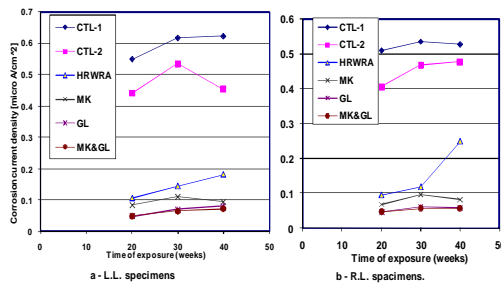


Figure (12) Corrosion Rates in the Immersed exposure Zone for all Specimens.

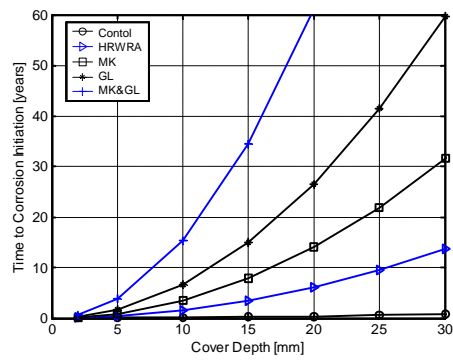


Figure (13) Predicted Time to Corrosion Initiation for All Specimens in Vertical Zone.